Optics & Laser Technology 41 (2009) 380–383

Contents lists available at ScienceDirect

Optics & Laser Technology

journal homepage: www.elsevier.com/locate/optlastec

Numerical and experimental analysis on green laser crystallization of amorphous silicon thin films

Zhijun Yuan *, Qihong Lou, Jun Zhou, Jingxing Dong, Yunrong Wei, Zhijiang Wang, Hongming Zhao, Guohua Wu

Shanghai Institute of Optics and Fine Mechanics, The Chinese Academy of Science, The Novel Laser Technique and Application System Laboratory, No.390, Qinghe Road, Jiading, Shanghai 201800, China

ARTICLE INFO

Article history:
Received 20 June 2008
Received in revised form
27 August 2008
Accepted 3 September 2008
Available online 23 October 2008

PACS:
79.20.Ds
73.61.−e
68.37.−d
78.30.−j

Keywords:
Thin film
Laser crystallization
Polycrystalline silicon
Finite difference simulation

ABSTRACT

The effect of laser fluence on the crystallization of amorphous silicon irradiated by a frequency-doubled Nd:YAG laser is studied both theoretically and experimentally. An effective numerical model is set up to predict the melting threshold and the optimized laser fluence for the crystallization of 200-nm-thick amorphous silicon. The variation of the temperature distribution with time and the melt depth is analyzed. Besides the model, the Raman spectra of thin films treated with different fluences are measured to confirm the phase transition and to determine the optimized fluence. The calculating results accord well with those obtained from the experimental data in this research.

© 2008 Elsevier Ltd. All rights reserved.

1. Introduction

Polycrystalline silicon (poly-Si) holds great potential for a number of applications, including thin-film transistors for active-matrix liquid-crystal displays (AMLCD) [1], sensors [2] and solar cells [3]. Laser crystallization of amorphous silicon (a-Si) is regarded as the most efficient method for fabricating polycrystalline silicon on glass [4]. However, the traditionally used excimer laser crystallization (ELC) has many disadvantages, such as the narrow process window of laser energy density, very high absorption of ultraviolet wavelength in a-Si and the costly maintenance. So in many recent works, green lasers, especially frequency-doubled Nd:YAG ($\lambda = 532$ nm), have been used instead of excimer lasers as the crystallization laser source [5–8].

Early experimental results revealed that the phase-change from a-Si to poly-Si depends strongly on the absorbed energy from the incident laser pulse [4]. However, the energy absorption and the temperature distribution in Si thin films are difficult to measure directly. So it is necessary and significant to make a theoretical analysis of the temperature field of the Si film when irradiated by pulsed laser. The heat transfer models for laser material processing have previously been reported and are used by some researchers for the simulation of ELC [9,10] or the laser interference crystallization [11]. But no systematic numerical study including the laser fluence effect on green laser crystallization has been reported.

According to Ref. [4], three main crystal-growth regimes (partial, near-complete and complete melting regimes) exist, depending on the laser fluence. Large grains can only be produced at the near-complete regime, which indicates a very narrow energy density window. The so-called “critical fluence” (F_c) [9] distinguishes between the partial melting regime and near-complete melting regime, indicating the optimized fluence for the crystallization of a-Si films. Hence, it is of great importance to determine the value of F_c.

In this work, the effect of laser fluence on green laser-induced crystallization of a-Si is investigated numerically and experimentally. The finite difference method is used to solve the heat conduction equation and to predict the value of the melting

* Corresponding author. Tel.: +86 021 69918629.
E-mail address: zhijunyuan@gmail.com (Z. Yuan).

0030-3992/$ - see front matter © 2008 Elsevier Ltd. All rights reserved.
doi:10.1016/j.optlastec.2008.09.003

threshold and of F_c. A laser crystallization experiment was also developed for fabricating poly-Si films. Results of the calculation are compared with experimental data of other researchers and our own in this work.

2. Mathematical model

When the pulsed laser irradiates the surface of silicon, only a fraction of the incident energy can be absorbed and taken as the heat source because of the effects of surface reflection. The temperature of the thin film begins to increase with the absorbed energy. The film melts to a liquid when the melt point (T_m) of a-Si is reached. Then it cools down and solidifies to polycrystalline phase after the irradiation.

The crystallization process of a-Si can be simulated with a one-dimensional non-linear heat conduction equation:

$$c(T)\rho\frac{\partial T}{\partial t}=\frac{\partial}{\partial x}\left[K(T)\frac{\partial T}{\partial x}\right]+S(x,t) \tag{1}$$

where c is the specific heat, ρ is the density, the temperature, $T(x, t)$, varies with depth x and time t, K is the thermal conductivity and $S(x, t)=S(x)S(t)$is the laser source term. The laser beam is assumed to be Gaussian shape, so the time-dependent part of the source term is given by

$$S(t)=\frac{1}{\Gamma\sqrt{\pi}}\exp-\left(\frac{t-t'}{\Gamma}\right)^2 \tag{2}$$

where Γ denotes the full-width duration of the pulse at $1/e$ intensity and t' is the time when the pulse reaches its maximum value.

$$S(x)=E_0(1-R_i)\alpha_i\exp(-\alpha_i x)\quad i=\mathrm{s\ or\ l} \tag{3}$$

where E_0 is the power density of the incident laser; R_i and α_i represent the reflectivity at the interface and the optical absorption coefficient of a-Si, respectively. Their value can be very different when the interface is solid phase (R_s, α_s) or liquid phase (R_l, α_l).

The specific heat c and the thermal conductivity K in Eq. (1) are generally temperature dependent, so it is difficult to solve the equation by the analytical approach. The finite difference method is used in this work to solve for $T(x,t)$, by dividing the irradiated region into equal sections of length Δx and time into equal sections of Δt. The expressions and values of the physical properties used in this simulation are shown in Table 1.

Initially, the temperature of a-Si is equal to the ambient temperature ($T_0=300$ K). So the boundary condition and initial condition are listed as follows:

$$T(x,t)|_{t=0}=T_0 \tag{4}$$

$$T(x,t)|_{x\to\infty}=T_0 \tag{5}$$

$$\left.\frac{\partial T(x,t)}{\partial x}\right|_{x=0}=0 \tag{6}$$

Table 1
Physical properties used in this simulation

Physical properties	Value or expression	Reference
Absorption coefficient (cm^{-1})	$\alpha_s=1.25\times10^5$; $\alpha_l=10^6$	[11]
Density (g/cm^3)	$\rho_s=2.20$; $\rho_l=2.53$	
Specific heat (J/g K)	$C(T)=0.952+0.171T/1685$	[10]
Reflectivity	$R_s=0.4$; $R_l=0.73$	[10,11]
Thermal conductivity (W/cm K)	$K(T)=4.828\times10^{-11}$ (T-900)3+4.828 $\times10^{-9}$ (T-900)2+3.714 $\times10^{-6}$ (T-900)+3.714 $\times10^{-2}$	[10]
Latent heat (J/g)	$L=1320$	[11]
Melting point of a-Si (K)	$T_m=1420$	[12,13]

Subscripts s and l denote the solid and liquid phase, respectively.

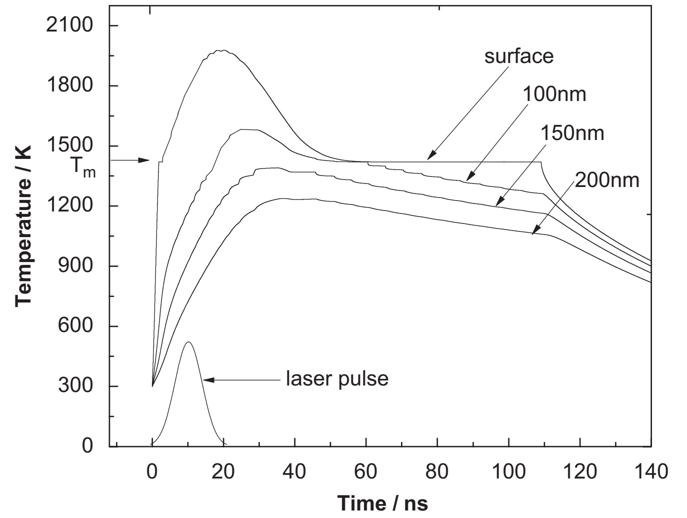

Fig. 1. Results of the simulation showing the temperature versus time profiles at the surface, 100, 150 and 200 nm layers of the 200 nm a-Si, which is irradiated by laser fluence of 600 mJ/cm^2.

The results of the modeling of the time-dependent temperature profile for a-Si:H thin film irradiated with a pulsed 2ωNd:YAG laser are shown in Fig. 1. The laser fluence is 600 mJ/cm^2. The shape of the laser pulse is also shown in the bottom left corner. The temperature at the surface rises rapidly until the melting point is reached. The surface begins to melt shortly after the pulse reaches its peak. When the surface layer is heated to the melt point T_m, the latent heat of melting must be considered. The temperature of the melting layer will remain at T_m until the energy of $\Delta Q=\rho L\Delta x$ is absorbed subsequently. Also, the latent heat should be taken into account when the liquid silicon release heat at the crystallization process.

The temperature profiles at depths 100, 150 and 200 nm are also plotted. It is noted that the temperature at the layer 200 nm below the surface is still lower than T_m. Therefore, a laser fluence of 600 mJ/cm^2 is not sufficient to melt the entire a-Si thin film of 200 nm. This is confirmed by our experiment, which will be discussed later.

There is an interest on how much laser fluence is required for a-Si crystallization. So the temperatures of surface and bottom layers irradiated by different laser fluences are calculated in Fig. 2. It can be seen that the maximum temperatures for both layers increase approximately linearly with laser fluence. As for an a-Si:H thin film of thickness 200 nm, the temperature of the surface layer reaches T_m when the laser fluence is about 210 mJ/cm^2, and the bottom layer begins melting only when laser fluence is over 800 mJ/cm^2. Then near-complete melting can be achieved.

The calculated threshold energy density for green laser crystallization, 210 mJ/cm^2, is about two times as much as that of ELC. This is mainly due to the reduced absorption of green light (1.25×10^5 cm^{-1}) in a-Si compared with that of ultraviolet light (1.43×10^6 cm^{-1}), so more energy is needed to reach the melting point.

3. Experiment procedure

A 500-nm-thick SiO_2 layer was deposited by Plasma-Enhanced Chemical Vapor Deposition (PECVD) on corning glass substrate, which acted as a thermal barrier. Then, a 200-nm-thick hydrogenated amorphous silicon (a-Si:H) film was deposited on the SiO_2 layer by PECVD of $SiH_4/SiCl_2H_2$. The gas pressure of the deposition was 67–133 Pa. Dehydrogenation of a-Si was done by a furnace annealing at 500 °C for 2 h.

A laser crystallization apparatus used in this work consisted of a 2ωYAG laser (532 nm) with 10-ns pulse width, a beam shaping system and a translation stage. The schematic diagram of our experiment is given in Fig. 3. The beam shaping system, including a fly-eye lens array, transformed the incoming Gaussian laser beam into a flattop one. A wave-front analyzer was used to examine the intensity uniformity on the image plane. The samples placed on the stage were scanned at a speed of 1.0 cm/s. After the crystallization, Raman spectra of thin films were measured by a Jobin Yvon LabRam-1B micro Raman spectrometer.

4. Results and discussion

Raman scattering measurements are performed to investigate the microstructure. As can be seen in Fig. 4, a sharp peak appears between 510 and 520 cm^{-1} after the laser treatment. That peak is assigned to the TO phonon scattering of poly-Si and resulted mainly from the phonon confinement effects [14], which indicates the phase transition from a-Si to poly-Si. The same TO peaks can be obtained by some other different crystallization techniques, such as ELC [15], low-pressure chemical vapor deposition [14] and so on.

Further investigation of the Raman spectra shows that laser fluence used in the irradiation of the thin films may exert a major influence on the shift and full-width at half-maximum (FWHM) of the TO peak. Fig. 5 shows the intensity-normalized Raman spectra of poly-Si crystallized using different energy densities .It can be seen that the asymmetric profile of the Raman spectra tends to be narrower and more symmetric when the laser fluence increased from 400 to 850 mJ/cm^2. Also, the TO peaks shift towards the frequency of 520 cm^{-1}, which is characteristic of crystalline silicon. This phenomenon indicates the enlargement of the grain size and crystalline percentage in the poly-Si thin films [15]. However, when the laser energy density is over 900 mJ/cm^2, the position of the TO peak begins to shift back.

In detail, the shift of the TO peaks at different laser fluences is shown in Fig. 6. The calculated melt depths of 200 nm a-Si from the heat conduction equations are also plotted.

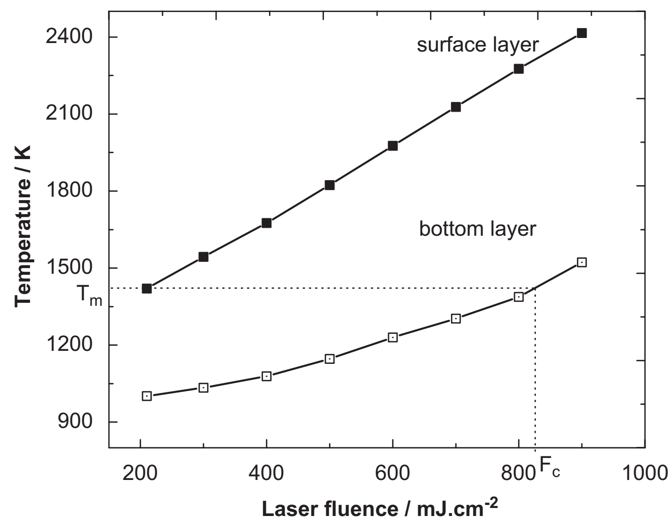

Fig. 2. Calculated maximum temperatures of the surface and bottom layers (200 nm below surface layer) at different laser fluences.

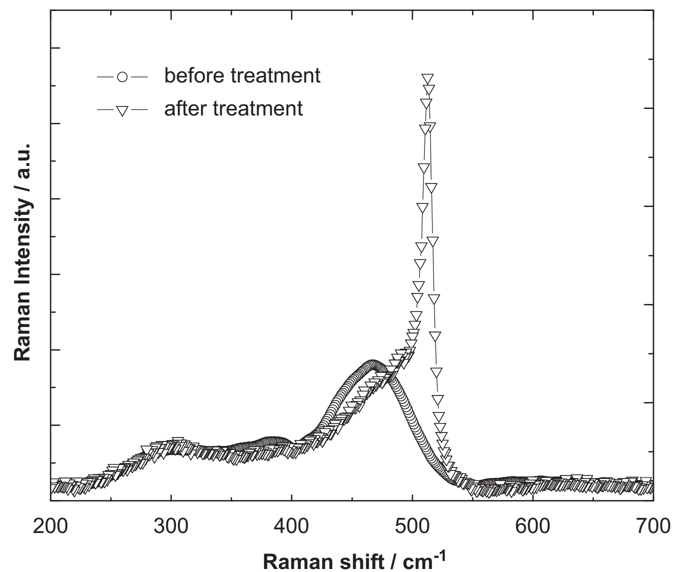

Fig. 4. Raman scattering spectra of a-Si before and after laser treatment.

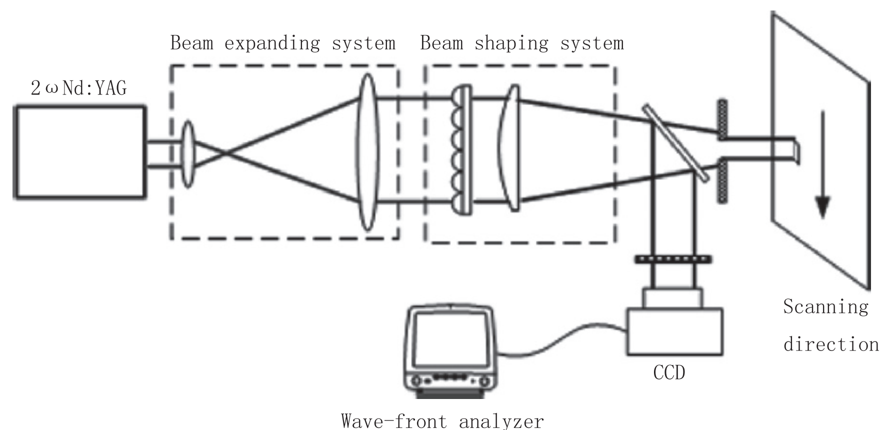

Fig. 3. Schematic diagram of laser crystallization.

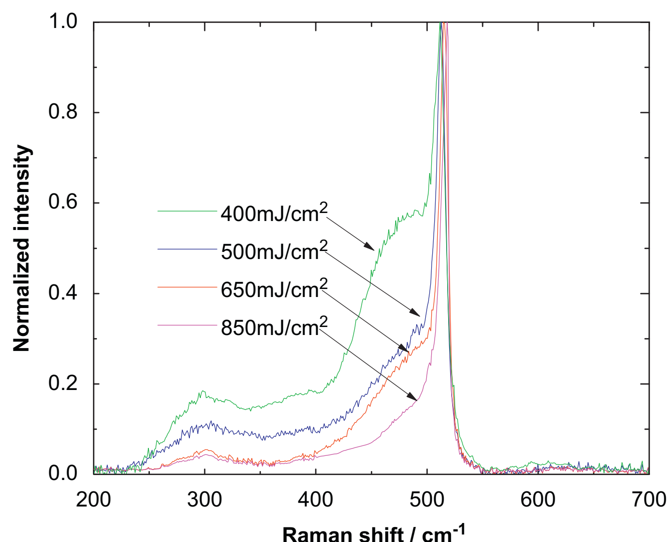

Fig. 5. Normalized Raman spectra of polycrystalline silicon crystallized by different laser fluences.

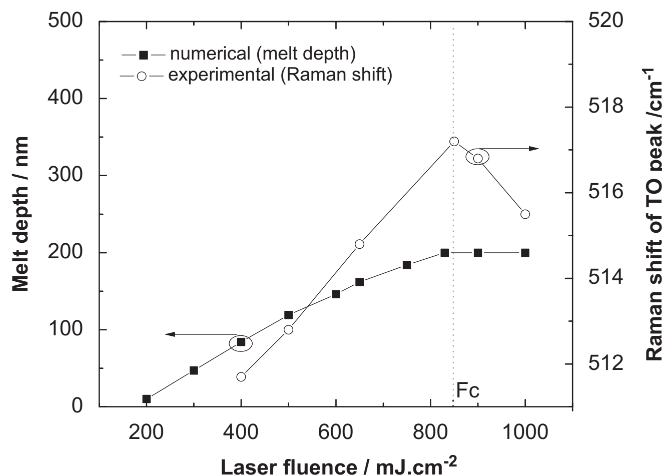

Fig. 6. Calculated melt depths and Raman shift of TO peaks versus laser fluence.

The critical F_c can be used to identify the partial and near-complete melting regimes. In Fig. 6, the fluence lower than F_c is in the partial melting regime. The calculated maximum melt depth is lower than the thickness of the Si film (200 nm) and it increases almost linearly with laser fluence. If the fluence is larger than F_c, the regime of complete melting is obtained and the melt depth remains constant with the thickness of the Si film. The near-complete melting occurs at the fluence lower than and near F_c; in this work, it is about 830 mJ/cm^2. On the other hand, in our experiment, the TO peaks in Raman spectra have the maximum shift when the fluence is about 850 mJ/cm^2. So from Fig. 6, the value of F_c obtained from the simulation results agrees fairly well with the experimental one.

5. Conclusions

In this paper, the green laser crystallization of a-Si is investigated numerically and experimentally. The model is used to predict the optimum laser parameters, including the threshold and critical fluence for crystallization. It also provides better understanding on the dynamics during the laser–material interaction process. The optimized critical fluence calculated by this model agrees well with that determined from Raman spectra. Near-complete melting is achieved by laser fluence of about 850 mJ/cm^2 in this work. In this region, the melt depth just approaches the thickness of the Si film and the largest grain size and crystalline fraction can be found.

References

[1] Brotherton SD. Polycrystalline silicon thin film transistors. Semicond Sci Technol 1995;10:721–38.

[2] Shah AV, Schade H, Vanecek M, Meier J, Vallat-Sauvain E, Wyrsch N, et al. Thin-film silicon solar cell technology. Prog Photovoltaics: Res Appl Technol 2004;12:113–42.

[3] Ecoffey S, Bouvetd, Ionescu A, Fazan P. Low-pressure chemical vapor deposition of nanograin polysilicon ultra-thin films. Nanotechnology 2002;13:290–3.

[4] Voutsas AT. A new era of crystallization: advances in polysilicon crystallization and crystal engineering. Appl Surf Sci 2003;208–209:250–62.

[5] Akito Hara, Fumiyo Takeuchi, Michiko Takei. High-performance polycrystalline silicon thin film transistors on non-alkali glass produced using continuous wave laser lateral crystallization. Jpn J Appl Phys 2002;41:L311–3.

[6] Dassow R, Kohler JR, Helen Y, Mourgues K, Bonnaud O, Mohammed-Brahim T, et al. Laser crystallization of silicon for high-performance thin-film transistors. Semicond Sci Technol 2000;15:L31–4.

[7] Seong Jin Park, Yu Mi Ku, Eun Hyun Kim, Jin Jang, Ki Hyung Kima, Chae Ok Kimb. Selective crystallization of amorphous silicon thin film by a CW green laser. J Non-Cryst Solids 2006;352:993–7.

[8] Saboundji A, Mohammed-Brahim T, Andrä G, Bergmann J, Falkb F. Thin film transistors on large single crystalline regions of silicon induced by cw laser crystallization. J Non-Cryst Solids 2004;338–340:758–61.

[9] Yu-Ru Chen, Chien-Hung Chang, Long-Sun Chao. Modeling and experimental analysis in excimer-laser crystallization of a-Si films. J Cryst Growth 2007;303:199–202.

[10] Ong CK, Tan HS, Sin EH. Calculations of melting threshold energies of crystalline and amorphous materials due to pulsed-laser irradiation. Mater Sci Eng 1986;79(11):79–85.

[11] Rezek B, Nebel CE, Stutzmann M. Laser beam induced currents in polycrystalline silicon thin films prepared by interference laser crystallization. J Appl Phys 2002;91(7):4220–8.

[12] Thompson MO, Galvin GJ, Mayer JW, Peercy PS, Poate JM, Jacobson DC, et al. Melting temperature and explosive crystallization of amorphous silicon during pulsed laser irradiation. Phys Rev Lett 1984;52(26):2360–3.

[13] Donovan EP, Spaepen F, Turnbull D, Poate JM, Jacobson DC. Heat of crystallization and melting point of amorphous silicon. Appl Phys Lett 1983;42(8):698–700.

[14] Voutsas AT, Hatalis MK. Raman spectroscopy of amorphous and microcrystalline silicon films deposited by low-pressure chemical vapor deposition. J Appl Phys 1995;78(12):6999–7006.

[15] Hecheng Zou, Liangcai Wu, Xinfan Huang, Feng Qiao, Peigao Han, Xiaohui Zhou, et al. Microstructure properties of nanocrystalline silicon/SiO_2 multilayers fabricated by laser-induced crystallization. Thin Solid Films 2005;491:212–6.